



Yasuhiro Yamaguchi · Hugo García-Tecocoatzi ·  
Alessandro Giachino · Atsushi Hosaka · Elena Santopinto ·  
Sachiko Takeuchi · Makoto Takizawa

# Heavy Hadronic Molecules Coupled with Multiquark States

Received: 10 May 2021 / Accepted: 26 May 2021 / Published online: 13 June 2021  
© The Author(s), under exclusive licence to Springer-Verlag GmbH Austria, part of Springer Nature 2021

**Abstract** We investigate the hidden-charm pentaquarks as a  $\Lambda_c \bar{D}^{(*)} - \Sigma_c^{(*)} \bar{D}^{(*)}$  hadronic molecule coupling to a compact five-quark state. The coupling to the compact state leads to an hadron short-range interaction generating an attraction. In addition, the one pion exchange potential (OPEP) as a long-range interaction is introduced by the Lagrangians satisfying the chiral and heavy quark spin symmetries. The OPEP has been known as a driving force to bind atomic nuclei, where the tensor term leading the coupled-channel effect generates a strong attraction. The mass degeneracy of heavy hadrons due to the heavy quark spin symmetry enhances the OPEP derived by the  $\pi D^{(*)} \bar{D}^{(*)}$  and  $\pi \Sigma_c^{(*)} \Sigma_c^{(*)}$  couplings. Introducing those interactions, we consistently explain the masses and widths of the  $P_c$  states reported by LHCb in 2019. The short range interaction has a dominant role to determine the energy-level structures, while the OPEP tensor term does the decay width.

## 1 Introduction

The exotic hadrons have aroused great interest in the nuclear and hadron physics. Their structures cannot be explained by the ordinary hadron picture, a baryon as a three-quark state and a meson as a quark-antiquark state, while the exotics have been considered to have multiquark components such as a compact multiquark, e.g.  $qq\bar{q}\bar{q}$  and  $qqqq\bar{q}$ , and a hadronic molecule being a hadron composite states, e.g. meson-meson and meson-baryon bound states. Recently many exotic states including a  $c\bar{c}$  component have been reported near the hadron thresholds. For the exotic meson sector, since the discovery of  $X(3872)$  in 2003 [1], many  $XYZ$

---

Y. Yamaguchi (✉)  
Advanced Science Research Center, Japan Atomic Energy Agency (JAEA), Tokai 319-1195, Japan  
E-mail: yamaguchi.yasuhiro@jaea.go.jp

H. G.-Tecocoatzi  
Department of Physics, University of La Plata (UNLP), 49 y 115 cc. 67, 1900 La Plata, Argentina

A. Giachino · E. Santopinto  
Istituto Nazionale di Fisica Nucleare (INFN), Sezione di Genova, Via Dodecaneso 33, 16146 Genova, Italy

A. Hosaka  
Research Center for Nuclear Physics (RCNP), Osaka University, Ibaraki, Osaka 567-0047, Japan

S. Takeuchi  
Japan College of Social Work, Kiyose, Tokyo 204-8555, Japan

M. Takizawa  
Showa Pharmaceutical University, Machida, Tokyo 194-8543, Japan

states found near the  $D^{(*)}\bar{D}^{(*)}$  thresholds have been investigated to understand their exotic natures theoretically and experimentally [2,3].

As the exotic baryon states, the Large Hadron Collider beauty experiment (LHCb) collaboration observed two hidden-charm pentaquarks,  $P_c(4380)$  and  $P_c(4450)$ , in  $\Lambda_b^0 \rightarrow J/\psi K^- p$  decay in 2015 [4]. This decay process indicates the  $P_c$  states have at least a five-quark content,  $uudc\bar{c}$ . The observation of the  $P_c$  states has motivated a lot of theoretical works, where various exotic structures of the  $P_c$  states have been discussed such as the compact pentaquarks,  $\Sigma_c^{(*)}\bar{D}^{(*)}$  hadronic molecules and the kinematic effects giving a non-resonant explanation [5–7].

In 2019, a new analysis has been reported using nine times more data from the Large Hadron Collider than the 2015 analysis [8]. The new analysis uncovers a complex structure of  $P_c(4450)$  that consists of two narrow separate peaks,  $P_c(4440)$  and  $P_c(4457)$ . A new resonance  $P_c(4312)$  is also found below the  $\Sigma_c\bar{D}$  threshold. For a broad  $P_c(4380)$ , however, the data can be fitted equally well without the Breit-Wigner contribution corresponding to  $P_c(4380)$ . To understand the structure of the observed state, more experimental and theoretical studies are needed.

The masses ( $M$ ) and widths ( $\Gamma$ ) of the  $P_c$  states are obtained by [4,8]

$$\begin{aligned} P_c(4312) : M &= 4311.9 \pm 0.7_{-0.6}^{+6.8}, \Gamma = 9.8 \pm 2.7_{-4.5}^{+3.7}, \\ P_c(4380) : M &= 4380 \pm 8 \pm 29, \Gamma = 205 \pm 18 \pm 86, \\ P_c(4440) : M &= 4440.3 \pm 1.3_{-4.7}^{+4.1}, \Gamma = 20.6 \pm 4.9_{-10.1}^{+8.7}, \\ P_c(4457) : M &= 4457.3 \pm 0.6_{-1.7}^{+4.1}, \Gamma = 6.4 \pm 2.0_{-1.9}^{+5.7}. \end{aligned}$$

These  $P_c$  states are reported near the hidden-charm meson-baryon thresholds. As mentioned above,  $P_c(4312)$  is found below the  $\Sigma_c\bar{D}$  threshold. The broad resonance  $P_c(4380)$  is below the  $\Sigma_c^*\bar{D}$  threshold. The twin peak  $P_c(4440)$  and  $P_c(4457)$  is obtained below the  $\Sigma_c\bar{D}^*$  threshold. The LHCb analysis in 2019 motivated new theoretical works (just to make some early works see [9–17]).

In the dynamics of heavy hadrons with a single heavy quark, the heavy quark spin symmetry (HQSS) is an essential one [3,18,19]. This symmetry appears in the heavy quark region, including charm ( $c$ ), bottom ( $b$ ) and top ( $t$ ) quarks. The suppression of the color magnetic interaction in the heavy quark limit ( $m_Q \rightarrow 0$ ) induces the HQSS realized as separation of the heavy quark spin and the total angular momentum of the light degrees of freedom, called a brown much. This suppression leads the mass degeneracy of heavy hadrons with different total angular momentum. For the case of a single heavy meson composed of a heavy quark  $Q$  and a light antiquark ( $\bar{q}$ ), masses of the vector meson ( $S = 1$ ) and pseudoscalar meson ( $S = 0$ ) are degenerate due to the HQSS, and these mesons belong to the same HQS multiplet. In the charmed hadrons, the approximate mass degeneracy has been found. The mass splitting of  $D$  and  $D^*$  mesons is about 140 MeV, while in the light quark sector, the mass splittings of  $\pi$  and  $\rho$ , and  $K$  and  $K^*$  are 630 MeV and 390 MeV, respectively, that are larger than that of  $D$  and  $D^*$ . The approximate mass degeneracy is also found in the charmed baryons  $\Sigma_c$  and  $\Sigma_c^*$ , where the mass splitting of  $\Sigma_c$  and  $\Sigma_c^*$  is about 65 MeV.

The small mass splittings of  $D$  and  $D^*$ , and  $\Sigma_c$  and  $\Sigma_c^*$  lead to the approximate degeneracy of the hidden-charm meson-baryon thresholds for the  $\Sigma_c\bar{D}$ ,  $\Sigma_c^*\bar{D}$ ,  $\Sigma_c\bar{D}^*$  and  $\Sigma_c^*\bar{D}^*$  channels. In addition the  $\Lambda_c\bar{D}^*$  thresholds are also close to the  $\Sigma_c^{(*)}\bar{D}^{(*)}$  thresholds. The  $\Lambda_c$  baryon does not belong to the HQS multiplet of  $\Sigma_c$  and  $\Sigma_c^*$ , while the mass splitting of  $\Lambda_c$  and  $\Sigma_c$  is not large, about 167 MeV. Hence there are six charmed meson-baryon thresholds,  $\Lambda_c\bar{D}$ ,  $\Lambda_c\bar{D}^*$ ,  $\Sigma_c\bar{D}$ ,  $\Sigma_c^*\bar{D}$ ,  $\Sigma_c\bar{D}^*$ , and  $\Sigma_c^*\bar{D}^*$ , around the reported  $P_c$  states. Thus the coupled-channel analysis for these meson-baryon channels is important to understand the dynamics around the  $\Lambda_c\bar{D}^{(*)} - \Sigma_c^{(*)}\bar{D}^{(*)}$  thresholds.

In this talk, we study the hidden-charm pentaquarks with coupling the  $\Lambda_c\bar{D}^{(*)} - \Sigma_c^{(*)}\bar{D}^{(*)}$  meson-baryon channels to the compact five-quark ( $5q$ ) states. The inclusion of the  $5q$  states is inspired by the quark cluster model calculations in Ref. [20]. The coupling to the  $5q$  states is introduced as the short range interaction between heavy meson and baryon as discussed in Refs. [21,22]. We also employ the one pion exchange potential (OPEP) derived from the interaction Lagrangians of a pion and heavy hadrons, satisfying the heavy quark spin and chiral symmetries. The OPEP has been known as the key ingredient in the nuclear force. In particular the OPEP tensor term produces a strong attraction, while the tensor operator induces channel couplings between states with different orbital angular momenta. By introducing the  $5q$  potential and the OPEP, we solve the coupled channel Schrödinger equations for the  $\Lambda_c\bar{D}^{(*)} - \Sigma_c^{(*)}\bar{D}^{(*)}$  channels. The channels considered in this study are summarised in Table 1.

**Table 1** The possible channels of the  $\Lambda_c \bar{D}^{(*)} - \Sigma_c^{(*)} \bar{D}^{(*)}$  states for given  $J^P$ 

$J^P$	Channels
$1/2^-$	$\Lambda_c \bar{D}^{(*)}(^2S), \Lambda_c \bar{D}^{(*)}(^2S, ^4D), \Sigma_c \bar{D}^{(*)}(^2S), \Sigma_c^{(*)} \bar{D}^{(*)}(^4D), \Sigma_c \bar{D}^{(*)}(^2S, ^4D), \Sigma_c^{(*)} \bar{D}^{(*)}(^2S, ^4D, ^6D)$
$3/2^-$	$\Lambda_c \bar{D}^{(*)}(^2D), \Lambda_c \bar{D}^{(*)}(^4S, ^2D, ^4D), \Sigma_c \bar{D}^{(*)}(^2D), \Sigma_c^{(*)} \bar{D}^{(*)}(^4S, ^4D), \Sigma_c \bar{D}^{(*)}(^4S, ^2D, ^4D), \Sigma_c^{(*)} \bar{D}^{(*)}(^4S, ^2D, ^4D, ^6D, ^6G)$
$5/2^-$	$\Lambda_c \bar{D}^{(*)}(^2D), \Lambda_c \bar{D}^{(*)}(^2D, ^4D, ^4G), \Sigma_c \bar{D}^{(*)}(^2D), \Sigma_c^{(*)} \bar{D}^{(*)}(^4D, ^4G), \Sigma_c \bar{D}^{(*)}(^2D, ^4D, ^4G), \Sigma_c^{(*)} \bar{D}^{(*)}(^6S, ^2D, ^4D, ^6D, ^4G, ^6G)$

The isospin is taken to be  $I = 1/2$ .  $^{2S+1}L$  in parenthesis stands for a total spin ( $S$ ) and an orbital angular momentum ( $L$ )

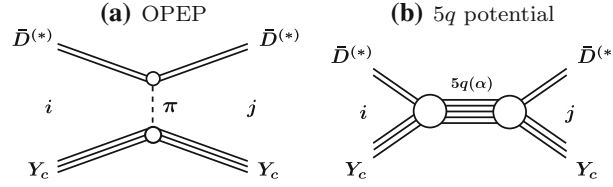


**Fig. 1** The **a** one pion exchange and **b**  $5q$  potentials between the  $\bar{D}^{(*)}$  meson and the  $Y_c = \Lambda_c, \Sigma_c^{(*)}$  baryon derived in [21,22].  $i$  and  $j$  stand for channels of the initial and final states, respectively.  $\alpha$  denotes a channel of the  $5q$  state

## 2 Hadron Interaction

We consider the hidden-charm hadronic molecules composed of  $\Lambda_c \bar{D}^{(*)}$  and  $\Sigma_c^{(*)} \bar{D}^{(*)}$  coupled to the compact five-quark state. As for the long-range hadron interaction, the OPEP is introduced, which has been known that the tensor term of the OPEP produces a significant attraction to bind atomic nuclei. The important role of the OPEP in the heavy hadron interactions has also been discussed, which is enhanced by the heavy quark spin symmetry [3,19,23]. The coupling to the five-quark state induces the short-range interaction ( $5q$  potential) between composite hadrons as shown in Fig. 1. The  $5q$  potential plays an attractive role because of the large masses of the five-quark state.

The OPEP is obtained as the Born term of the  $t$ -channel diagram with the pion exchange process. The diagram is given by the effective Lagrangians of a pion and heavy hadrons,  $\bar{D}^{(*)}$  mesons and  $\Lambda_c, \Sigma_c^{(*)}$  baryons, satisfying the heavy quark spin and chiral symmetries.

The Lagrangians of a pion and  $\bar{D}^{(*)}$  mesons are written by [3,18,24]

$$\mathcal{L}_{\pi HH} = g_A^M \text{Tr} [H_b \gamma_\mu \gamma_5 A_{ba}^\mu \bar{H}_a], \quad (1)$$

where the heavy meson field  $H_a$  containing the heavy quark spin multiplet of pseudoscalar and vector fields  $\bar{D}_a$  and  $\bar{D}_a^\mu$  as

$$H_a = [\bar{D}_{a\mu}^* \gamma^\mu - \bar{D}_a \gamma_5] \frac{1 + \not{v}}{2}, \quad (2)$$

$$\bar{H}_a = \gamma_0 H_a^\dagger \gamma_0, \quad (3)$$

with the subscript  $a, b$  denoting the light quark flavor. The trace is taken over the gamma matrices.  $v^\mu$  is the four-velocity of the heavy quark inside the heavy hadron. The coupling constant  $g_A^M$  is determined by the  $D^* \rightarrow D\pi$  decay as  $g_A^M = 0.59$ .  $A_{ba}^\mu$  is the axial-vector current given by

$$A^\mu = \frac{i}{2} [\xi^\dagger \partial_\mu \xi - \xi \partial_\mu \xi^\dagger], \quad (4)$$

$$\xi = \exp\left(\frac{i\hat{\pi}}{2f_\pi}\right), \quad \hat{\pi} = \begin{pmatrix} \pi^0 & \sqrt{2}\pi^+ \\ \sqrt{2}\pi^- & -\pi^0 \end{pmatrix}, \quad (5)$$

where the pion decay constant  $f_\pi = 93$  MeV.

The Lagrangians of a pion and heavy baryons  $\Lambda_c$  and  $\Sigma_c^{(*)}$  are written by [25,26]

$$\mathcal{L}_{\pi Y_c Y_c} = \frac{3}{2} i g_1 \varepsilon^{\mu\nu\lambda\kappa} v_\kappa \text{tr} [\bar{S}_\mu A_\nu S_\lambda] + g_4 \text{tr} [\bar{S}_\mu A_\mu \hat{\Lambda}_c] + H.c., \quad (6)$$

where the heavy baryon field is given by

$$S_\mu = \hat{\Sigma}_{c\mu}^* - \frac{1}{\sqrt{3}} (\gamma_\mu + v_\mu) \gamma_5 \hat{\Sigma}_c, \quad (7)$$

$$\hat{\Lambda}_c = \begin{pmatrix} 0 & \Lambda_c^+ \\ -\Lambda_c^\dagger & 0 \end{pmatrix}, \quad \hat{\Sigma}_{c(\mu)}^{(*)} = \begin{pmatrix} \Sigma_{c(\mu)}^{(*)++} & \frac{1}{\sqrt{2}} \Sigma_{c(\mu)}^{(*)+} \\ \frac{1}{\sqrt{2}} \Sigma_{c(\mu)}^{(*)+} & \Sigma_{c(\mu)}^{(*)0} \end{pmatrix}. \quad (8)$$

We take  $g_A^B \equiv g_1 = (\sqrt{8}/3)g_4 = 1$  estimated by the quark model calculation.

From the Lagrangians in Eqs. (1) and (6), the OPEP in the momentum space is obtained as

$$V_{ij}^\pi(\mathbf{q}) = \left( \frac{g_A^M g_A^B}{4f_\pi^2} \right) \frac{1}{3} \left[ \mathbf{S}_1^{(ij)} \cdot \mathbf{S}_2^{(ij)} \frac{m_\pi^2}{\mathbf{q}^2 + m_\pi^2} + S_{12}(\hat{q}) \frac{-\mathbf{q}^2}{\mathbf{q}^2 + m_\pi^2} \right] F_M(\mathbf{q}) F_B(\mathbf{q}). \quad (9)$$

$\mathbf{S}_1^{(ij)}$  and  $\mathbf{S}_2^{(ij)}$  are the spin operator for mesons and baryons, respectively, which depends on the initial ( $i$ ) and final ( $j$ ) states. The tensor operator  $S_{12}(\hat{q})$  is defined as  $S_{12}(\hat{q}) = 3(\mathbf{S}_1 \cdot \hat{q})(\mathbf{S}_2 \cdot \hat{q}) - \mathbf{S}_1 \cdot \mathbf{S}_2$ .  $F_M(\mathbf{q})$  and  $F_B(\mathbf{q})$  are the form factor of the meson and baryon, respectively, introducing to take into account a finite size of the hadron,

$$F_H(\mathbf{q}) = \frac{\Lambda_H^2 - m_\pi^2}{\Lambda_H^2 + \mathbf{q}^2}, \quad (10)$$

where  $H = M, B$ .  $\Lambda_H$  is the cutoff parameter determined by the hadron size  $r_H$  and the ratio  $\Lambda_N/\Lambda_H = r_H/r_N$  with the nucleon size and cutoff,  $r_N$  and  $\Lambda_N$  [21,22,27]. The hadron sizes are estimated by the quark model. We obtain the heavy hadron cutoffs as  $\Lambda_{\bar{D}^{(*)}} = 1.35\Lambda_N$  and  $\Lambda_{Y_c} = \Lambda_N$ . The nucleon cutoff is given by  $\Lambda_N = 837$  MeV to reproduce the deuteron binding energy when the OPEP is employed.

The coupling between the meson-baryon molecules and five-quark states leads to the short-range interaction,

$$V_{ij}^{5q} = \sum_\alpha \langle i|V|\alpha\rangle \frac{1}{E - E_\alpha^{5q}} \langle \alpha|V^\dagger|j\rangle, \quad (11)$$

where  $i, j$  denote the meson-baryon ( $MB$ ) channel, while  $\alpha$  the  $5q$  channel as summarized in Table 2.  $V$  is the transition potential between the  $MB$  and  $5q$  channels.  $E_\alpha^{5q}$  is the eigen energy of the  $5q$  channel, estimated by the quark model calculation [21] as summarized in Table 3. The obtained  $E_\alpha^{5q}$ s are several hundred MeV above the thresholds we are interested such as  $\Sigma_c^* \bar{D}^* \sim 4527$  MeV. Thus we reduce the  $5q$  potential in Eq. (11) to the simple contact interaction,

$$V_{ij}^{5q}(r) = -f \sum_\alpha S_i^\alpha S_j^\alpha e^{-Ar^2}. \quad (12)$$

The strength  $f$  is a free parameter that is determined from the experimental data for the  $P_c$  states.  $S_i^\alpha$  is the spectroscopic factor obtained by the overlap of the color-flavor-spin wave functions of the  $MB$  and  $5q$  states, that is summarized in Table 4. We consider that the  $5q$  potential generates an attraction. Since the masses of the compact  $5q$  states are larger than the  $Y_c \bar{D}^{(*)}$  threshold energies, namely  $E_\alpha^{5q} > m_{Y_c} + m_{\bar{D}^{(*)}}$ , the  $5q$  potential plays an attractive role due to the level repulsion. We introduce the Gaussian form factor in the  $5q$  potential. The Gaussian parameter  $A$  should be proportional to the inverse of the distance between  $cqq$  and  $\bar{c}q$  clusters inside the compact  $5q$  state. We assume that the distance is less than 1 fm, and  $A = 1 \text{ fm}^{-1}$  is employed in this study.

**Table 2** Channels of the  $5q$  states for given  $J^P$ 

$J^P$	Channels
$1/2^-$	$[0 \otimes 1/2], [1 \otimes 1/2], [1 \otimes 3/2]$
$3/2^-$	$[0 \otimes 3/2], [1 \otimes 1/2], [1 \otimes 3/2]$
$5/2^-$	$[1 \otimes 3/2]$

The spin configurations are represented by  $[S_{c\bar{c}} \otimes S_{3q}]$  with the  $c\bar{c}$  spin ( $S_{c\bar{c}}$ ) and the total light-quark spin ( $S_{3q}$ )

**Table 3** Masses of the compact five-quark states obtained by the quark model calculations [21]

$J^P$	$[0 \otimes 1/2]$	$[1 \otimes 1/2]$	$[0 \otimes 3/2]$	$[1 \otimes 3/2]$
$1/2^-$	4816.2	4759.1	–	4772.2
$3/2^-$	–	4822.3	4892.5	4835.4
$5/2^-$	–	–	–	4940.7

**Table 4** The spectroscopic factors of the  $5q$  potential for given a total angular momentum  $J$ , a total  $c\bar{c}$  spin  $S_{c\bar{c}}$ , and a total light-quark spin  $S_{3q}$ 

$J$	$S_{c\bar{c}}$	$S_{3q}$	$\Lambda_c \bar{D}$	$\Lambda_c \bar{D}^*$	$\Sigma_c \bar{D}$	$\Sigma_c^* \bar{D}$	$\Sigma_c \bar{D}^*$	$\Sigma_c^* \bar{D}^*$
$1/2$	0	$1/2$	0.35	0.61	–0.35	–	0.20	–0.58
	1	$1/2$	0.61	–0.35	0.20	–	–0.59	–0.33
	1	$3/2$	0.00	0.00	–0.82	–	–0.47	0.33
$3/2$	0	$3/2$	–	0.00	–	–0.50	0.58	–0.65
	1	$1/2$	–	0.71	–	0.41	–0.24	–0.53
	1	$3/2$	–	0.00	–	–0.65	–0.75	–0.17
$5/2$	1	$5/2$	–	–	–	–	–	–1.00

The values are taken from [21]

### 3 Numerical Results

Resonances of the meson-baryon systems are obtained by solving the Schrödinger equation,

$$\left( K + V^\pi(r) + V^{5q}(r) \right) \psi(r) = E \psi(r) \quad (13)$$

where  $K$ ,  $V^\pi(r)$  and  $V^{5q}(r)$  stand for the kinetic term, the OPEP and the  $5q$  potential respectively.  $\psi(r)$  is the wave function of the meson-baryon systems that is described by the Gaussian expansion method [28]. To obtain the resonance energy and decay width, the complex scaling method [29–32] is applied.

Firstly we determine the free parameter  $f$  in Eq. (12). By tuning the parameter as  $f = 480$  MeV, we obtain resonances whose masses and widths are consistent with those of  $P_c(4312)$ ,  $P_c(4440)$  and  $P_c(4457)$  reported by the LHCb collaboration. The total angular momentum and parity of those  $P_c$ 's are assigned as  $J^P = 1/2^-$ ,  $3/2^-$  and  $1/2^-$  for  $P_c(4312)$ ,  $P_c(4440)$  and  $P_c(4457)$ , respectively.

Using  $f = 480$  MeV, we also obtain resonances near the  $Y_c \bar{D}^{(*)}$  thresholds in addition to the state corresponding to the  $P_c$ 's, as shown in Fig. 2. Below the  $\Sigma_c^* \bar{D}$  threshold, the resonance for  $J^P = 3/2^-$  is obtained, and the mass, being 4350 MeV, is close to the one of  $P_c(4380)$ . However the broad width of  $P_c(4380)$  that is more than 200 MeV is not explained by this calculation with the narrow width. Further theoretical and experimental studies are necessary to understand the nature of  $P_c(4380)$ .

Furthermore three resonances are found below the  $\Sigma_c^* \bar{D}^*$  threshold. The masses ( $J^P$ ) are obtained as 4521 MeV ( $J^P = 1/2^-$ ), 4511 MeV ( $J^P = 3/2^-$ ) and 4468 MeV ( $J^P = 5/2^-$ ).

To examine the role of the interactions, we compare the results with and without the OPEP tensor term. The results near the  $\Sigma_c \bar{D}^*$  and  $\Sigma_c^* \bar{D}^*$  thresholds are shown in Fig. 3. From this figure, we find the following interesting observations.

- (1) The  $5q$  potential plays a dominant role to generate the attraction determining the energy level.
- (2) The OPEP tensor term produces the attraction, and has a significant role in the decay widths.

In Fig. 3, switching off the OPEP tensor force does not change the order of the energy level. It indicates that the  $5q$  potential predominates the energy-level structure of the meson-baryon resonances. The level order

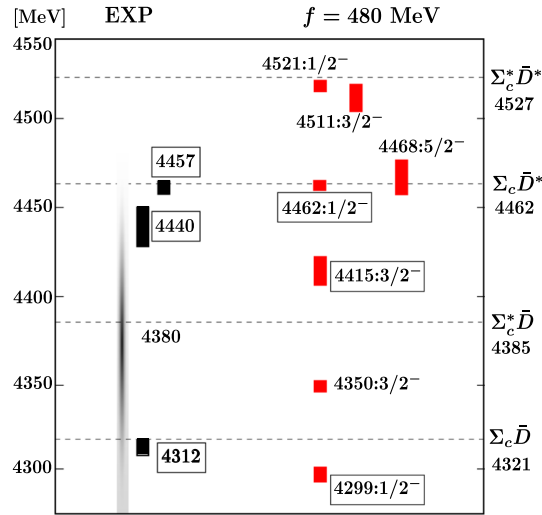


**Fig. 2** Experimental data in LHCb (EXP) and our prediction with  $f = 480$  MeV [22]. The centers of the boxes are located at the central values of pentaquark masses, while their lengths correspond to the widths (except for the broad  $P_c(4380)$ ). The horizontal dashed lines show the meson-baryon thresholds

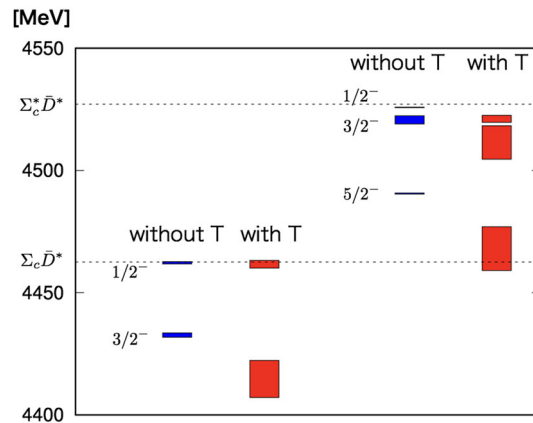


**Fig. 3** Comparison between the results with and without the OPEP tensor force near the  $\Sigma_c \bar{D}^*$  and  $\Sigma_c^* \bar{D}^*$  thresholds [22]

is determined by the spectroscopic factor in the  $5q$  potential given by the color-flavor-spin structure of the compact  $5q$  states.

The role of the OPEP tensor force is enhanced by the coupled-channel effect. The tensor force produces the attraction because it contributes to the energy in the second order perturbation. In Fig. 3 we find that the attractive force due to the tensor force increases as the total angular momentum  $J$  becomes larger. The results in Fig. 3 also show the important role of the tensor force in the decay widths. The very narrow widths are obtained without the tensor force. Thanks to the tensor operator and the heavy quark spin symmetry, many meson-baryon channels can couple to the resonances. The coupling to the channels below the resonances is important to produce the width, that is enhanced by the coupled-channel effect.

## 4 Summary

We investigate the masses and decay widths of hidden-charm pentaquarks. The candidates of pentaquarks were reported by the LHCb collaboration as the  $P_c$  states. We consider the coupling the open-charm meson-baryon channels to a compact five-quark ( $qqqc\bar{c}$ ) core. As for the hadron interaction, the OPEP as the long range force, and the  $5q$  potential as the short range one are employed. The OPEP is obtained the interaction Lagrangians satisfying the heavy quark and chiral symmetries, and the significant role of the tensor term has been known in the nuclear force. The  $5q$  potential is introduced as the contact interaction derived from the coupling the

$Y_c \bar{D}^{(*)}$  channels to the  $5q$  states. The color-flavor-spin structures of the  $5q$  state are taken into account as the spectroscopic factor. For the three  $P_c$  states reported by LHCb, both the masses and widths we obtained are in reasonable agreement with the experimental results. The quantum numbers  $J^P$  for the  $P_c$  states are obtained as  $J^P = 1/2^-$  for  $P_c(4312)$ ,  $J^P = 3/2^-$  for  $P_c(4440)$ , and  $J^P = 1/2^-$  for  $P_c(4457)$ . Below the  $\Sigma_c^* \bar{D}$  threshold, we find a resonance for  $J^P = 3/2^-$ . The mass is consistent with the one of the broad  $P_c(4380)$ , while the decay width is very narrow. Moreover, three resonances for  $J^P = 1/2^-, 3/2^-, 5/2^-$  are found below the  $\Sigma_c^* \bar{D}^*$  threshold. The role of the interaction is studied. We find that the  $5q$  potential plays a major role in determining of the ordering of the resonances, while the OPEP tensor force does in producing the decay widths.

**Acknowledgements** This work is supported in part by JSPS KAKENHI Grant Numbers JP20K14478 (Y.Y.), JP16K05361(C) (S.T. and M.T.), JP17K05441 (C), and Grants-in-Aid for Scientific Research on Innovative Areas (No.18H05407) (A.H.). This work is also supported in part by the “RCNP Collaboration Research network (COREnet)”.

## References

1. S.K. Choi et al., Phys. Rev. Lett. **91**, 262001 (2003)
2. N. Brambilla et al., Eur. Phys. J. C **71**, 1534 (2011)
3. Y. Yamaguchi, A. Hosaka, S. Takeuchi, M. Takizawa, J. Phys. G **47**(5), 053001 (2020)
4. R. Aaij et al., Phys. Rev. Lett. **115**, 072001 (2015)
5. H.X. Chen, W. Chen, X. Liu, S.L. Zhu, Phys. Rep. **639**, 1 (2016)
6. A. Esposito, A. Pilloni, A.D. Polosa, Phys. Rep. **668**, 1 (2017)
7. A. Ali, J.S. Lange, S. Stone, Prog. Part. Nucl. Phys. **97**, 123 (2017)
8. R. Aaij et al., Phys. Rev. Lett. **122**, 222001 (2019)
9. C.W. Xiao, J. Nieves, E. Oset, Phys. Rev. D **100**, 014021 (2019)
10. M.Z. Liu, Y.W. Pan, F.Z. Peng, M.S. Sánchez, L.S. Geng, A. Hosaka, M.P. Valderrama, Phys. Rev. Lett. **122**, 242001 (2019)
11. Y. Shimizu, Y. Yamaguchi, M. Harada, [arXiv:1904.00587](https://arxiv.org/abs/1904.00587) [hep-ph] (2019)
12. F. Giannuzzi, Phys. Rev. D **99**, 094006 (2019)
13. J.F. Giron, R.F. Lebed, C.T. Peterson, JHEP **05**, 061 (2019)
14. J. He, Eur. Phys. J. C **79**(5), 393 (2019)
15. A. Ali, A.Y. Parkhomenko, Phys. Lett. B **793**, 365 (2019)
16. Z.H. Guo, J.A. Oller, Phys. Lett. B **793**, 144 (2019)
17. T.J. Burns, E.S. Swanson, Phys. Rev. D **100**, 114033 (2019)
18. A.V. Manohar, M.B. Wise, *Heavy Quark Physics*. Cambridge Monographs on Particle Physics, Nuclear Physics and Cosmology (Cambridge University Press, 2000)
19. A. Hosaka, T. Hyodo, K. Sudoh, Y. Yamaguchi, S. Yasui, Prog. Part. Nucl. Phys. **96**, 88 (2017)
20. S. Takeuchi, M. Takizawa, Phys. Lett. B **764**, 254 (2017)
21. Y. Yamaguchi, A. Giachino, A. Hosaka, E. Santopinto, S. Takeuchi, M. Takizawa, Phys. Rev. D **96**(11), 114031 (2017)
22. Y. Yamaguchi, H. García-Tecocoatzí, A. Giachino, A. Hosaka, E. Santopinto, S. Takeuchi, M. Takizawa, Phys. Rev. D **101**(9), 091502 (2020)
23. S. Yasui, K. Sudoh, Phys. Rev. D **80**, 034008 (2009)
24. R. Casalbuoni, A. Deandrea, N. Di Bartolomeo, R. Gatto, F. Feruglio, G. Nardulli, Phys. Rep. **281**, 145 (1997)
25. T.M. Yan, H.Y. Cheng, C.Y. Cheung, G.L. Lin, Y.C. Lin, H.L. Yu, Phys. Rev. D **46**, 1148 (1992). [Erratum: Phys.Rev.D 55, 5851 (1997)]
26. Y.R. Liu, M. Oka, Phys. Rev. D **85**, 014015 (2012)
27. Y. Yamaguchi, S. Ohkoda, S. Yasui, A. Hosaka, Phys. Rev. D **84**, 014032 (2011)
28. E. Hiyama, Y. Kino, M. Kamimura, Prog. Part. Nucl. Phys. **51**, 223 (2003)
29. J. Aguilar, J.M. Combes, Commun. Math. Phys. **22**(4), 269 (1971)
30. E. Balslev, J.M. Combes, Commun. Math. Phys. **22**(4), 280 (1971)
31. B. Simon, Commun. Math. Phys. **27**(1), 1 (1972)
32. S. Aoyama, T. Myo, K. Katō, K. Ikeda, Prog. Theor. Phys. **116**(1), 1 (2006)

**Publisher’s Note** Springer Nature remains neutral with regard to jurisdictional claims in published maps and institutional affiliations.